

AR-009-768

DSTO-TN-0048

D

S

F

High Frequency Bottom Back
Scattering in the Darwin Area

M.J. Bell

DTIC QUALITY INSPECTED 4

APPROVED FOR PUBLIC RELEASE

© Commonwealth of Australia

19970307 051

DEPARTMENT OF DEFENCE
DEFENCE SCIENCE AND TECHNOLOGY ORGANISATION

THE UNITED STATES NATIONAL
TECHNICAL INFORMATION SERVICE
IS AUTHORISED TO
REPRODUCE AND SELL THIS REPORT

High Frequency Bottom Back Scattering in the Darwin Area

M. J. Bell

**Maritime Operations Division
Aeronautical and Maritime Research Laboratory**

DSTO-TN-0048

ABSTRACT

The backscatter of acoustic energy from the sea floor has been measured at acoustic frequencies of 34 kHz, 100 kHz and 205 kHz. Measurements made at several sites near Darwin are reported. Measurements were made as a function of grazing angle and azimuth. During the experiments site environmental measurements were made to characterise in detail the area of the acoustic measurements. The locations, equipment and techniques used during the measurements are described.

RELEASE LIMITATION

Approved for public release

DEPARTMENT OF DEFENCE

DEFENCE SCIENCE AND TECHNOLOGY ORGANISATION

Published by

*DSTO Aeronautical and Maritime Research Laboratory
PO Box 4331
Melbourne Victoria 3001*

*Telephone: (03) 9626 8111
Fax: (03) 9626 8999
© Commonwealth of Australia 1996
AR No. AR-009-768
August 1996*

APPROVED FOR PUBLIC RELEASE

High Frequency Bottom Back Scattering in the Darwin Area

Executive Summary

Active sonars detect contacts by transmitting sound energy into the ocean and listening for echoes. When the echo is above the background noise level detections can be made. For minehunting sonars the background noise is usually dominated by sound energy from the transmission which has been reflected back from the sea bottom to the receiver. This is known as bottom reverberation. The level of bottom reverberation depends on the reflection coefficient or back-scattering strength of the bottom.

This document describes equipment, procedures and results from experiments conducted near Darwin to measure bottom backscattering strength at minehunting sonar frequencies.

Contents

1. INTRODUCTION	1
2. LOCATION.....	2
3. EQUIPMENT	4
4. EXPERIMENTS	5
4.1 Experiment Procedure.....	5
4.2 Data Analysis.....	6
5. RESULTS.....	7
5.1 Variation of bottom backscattering strength with grazing angle.....	7
5.2 Frequency Dependence	25
5.3 Variation with Azimuth.	25
5.4 Bottom Characterization.....	26
6. CONCLUSION.....	27
7. REFERENCES.....	28

1. Introduction

Bottom backscatter is the sound scattered back to the source by scatterers on or near the sea bottom. It is of particular importance in minehunting sonars as it generally forms the background signal against which the sonar must detect mines and mine-like objects.

The basic mechanisms of bottom backscattering are not completely understood and current environmental acoustic scattering models [1] are deficient in their capability to reliably predict bottom backscattering strength. Backscattering from the sea floor at shallow grazing angles is broadly correlated with the bottom type classifications of mud, sand, gravel and rock; however, within these bottom categories significant variations in backscattering strengths occur and knowledge of sediment type is in itself insufficient to predict backscatter strength. Until such time that the physical processes are properly characterised, at sea measurements of bottom backscatter are unavoidable if accurate estimates of backscatter from the sea floor are required.

The first significant report of experimentally determined bottom backscattering strength was published by McKinney and Anderson [2] almost 30 years ago. Since that time several authors including Boehme *et al.* [3,4], Jackson *et al.* [5], and Stannic *et al.* [6,7] have reported experimentally determined bottom backscattering strengths over a range of bottom types and locations. The data show trends that are consistent within a broad general framework; however significant variation exists.

As part of its support program for the Mine Hunter Coastal (MHC) project, Maritime Operations Division of the Aeronautical and Maritime Research Laboratory, conducted a series of bottom backscatter measurements in March 1993 in Beagle Gulf north of Darwin. This document collates and reports bottom back scattering data from those experiments.

Backscatter experiments were conducted at the frequencies 34 kHz, 100 kHz and 204 kHz; over a range of bottom grazing angles from about 2° to 40°. This frequency range embraces the detection frequencies of current RAN minehunting sonars and sonars under consideration for the proposed MHC vessels.

The measurements were made with transducer pairs mounted on top of a 4 metre high tower structure that rested on the bottom. A pan and tilt mechanism, remotely controlled by shipboard personnel, allowed variation in elevation and azimuth. Environmental measurements conducted in support of the bottom backscatter experiments included side-scan sonar survey, sound speed profiles, sediment samples and stereo bottom photography. The equipment and procedures are developments of those reported previously by Lawrence *et al* [8].

2. Location

The experiment sites were RAN exercise areas 207 and 214 in the Beagle Gulf north of Darwin. Area 207 was about 25 miles north of Darwin at the western edge of Moresby Shoals, while area 214 was about 40 miles west of Darwin. The water depth in Area 207 south of Melville Island was approximately 28 metres. In Area 214 it was close to 38 metres.

These areas were defined by co-ordinates:

AREA 207	12° 00'S, 130° 38'E	12° 00'S, 130° 43'E
	12° 04'S, 130° 38'E	12° 04'S, 130° 43'E
AREA 214	12° 15'S, 130° 05'E	12° 15'S, 130° 10'E
	12° 18'S, 130° 05'E	12° 18'S, 130° 10'E

Areas 207 and 214, and their relationship to Darwin are shown on the map in figure 1.

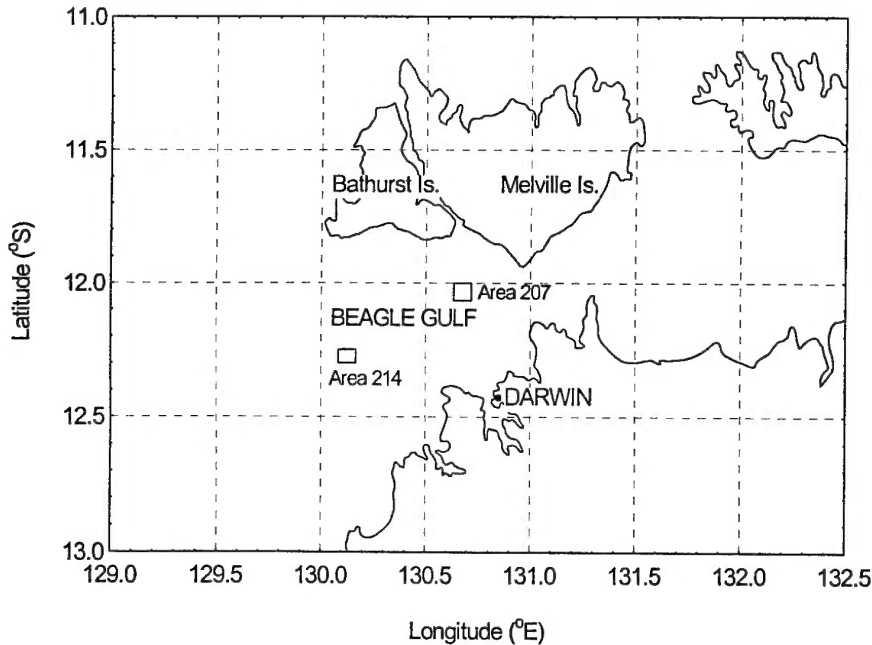


Figure 1. Location of experiment areas for MOD cruise SS2/93.

Side scan sonar surveys were conducted prior to the bottom reverberation measurements to identify variations in bottom characteristics and bathymetry, and to identify suitable sites. These surveys showed the western side of each area to be populated with sand ridges and undulations. The experiment sites were therefore chosen in the eastern side of each area.

Location of Experiment Sites - Area 207

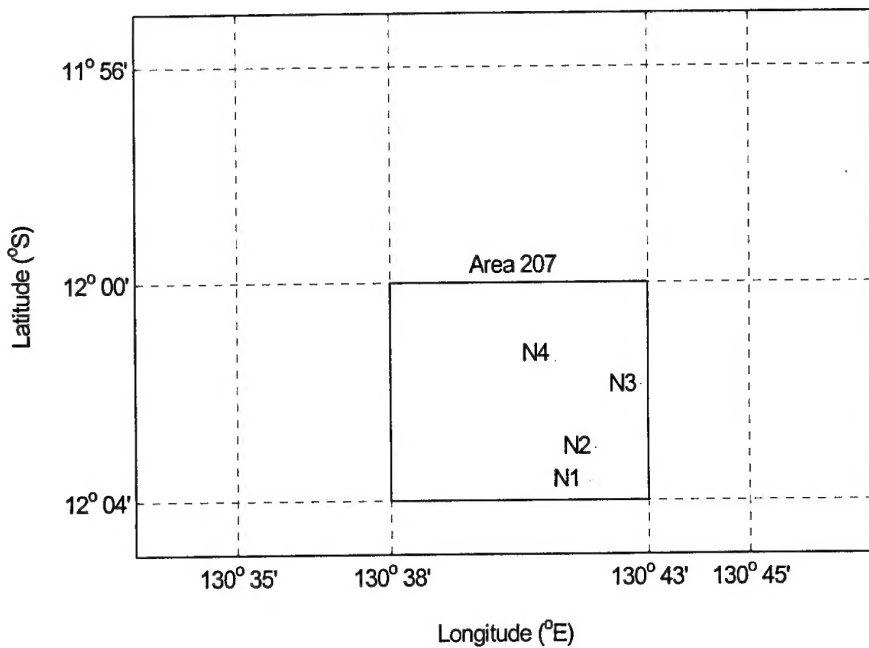


Figure 2A. Locations of experiment sites in area 207.

Four sites were occupied in each area. N1, N2, N3 and N4 in Area 207; and W1, W2, W3 and W4 in Area 214. These stations are indicated on the diagrams for areas 207 and 214 in figures 2A and 2B. Due to equipment malfunction no data was recorded at site N2.

Location of Experiment Sites - Area 214

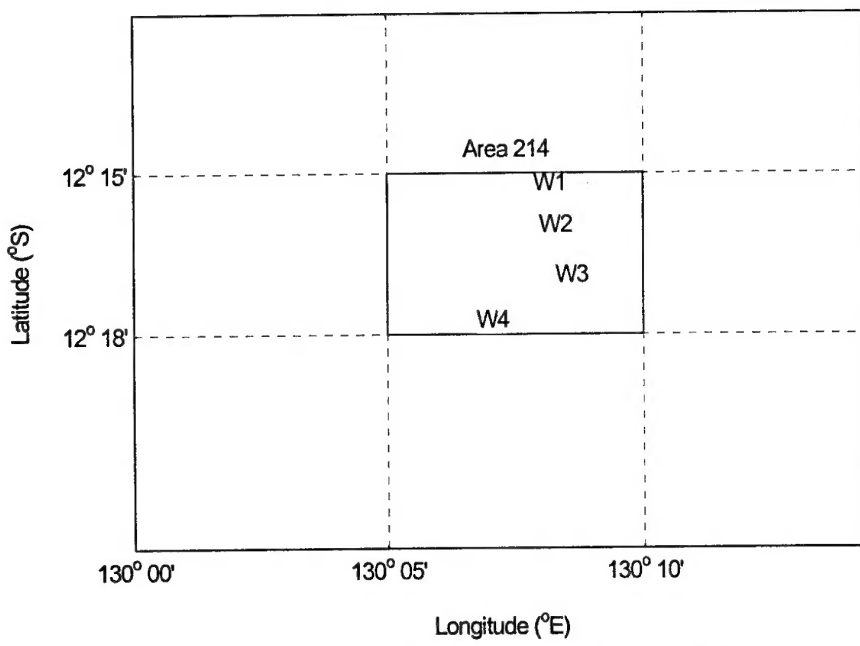


Figure 2B. Locations of experiment sites in area 214.

In southern latitudes early March is the middle of the oceanographic summer. Consequently, sea temperatures were near the annual maximum, and at some stations exceeded 29°C. Throughout the experiment period tidal currents up to two knots prevailed, and equipment bottom time was restricted by these tidal streams to less than 5 hours. The time window extended from about one hour after slack water, by which time the current direction had stabilised, to about half an hour before the next slack water when the current direction began to veer rapidly (although the current was weak) and the ship began to swing.

3. Equipment

The measurement structure was a tower with a transducer array mounted at the top on a pan and tilt mechanism. This allowed the transducers to be trained in elevation and azimuth. The centre of the transducer array was 4.08 metres above the sea floor. The underwater electronics package for controlling the experiment and collecting the data was mounted within the tower and connected by an electrical umbilical to shipboard electronics; thus permitting control of azimuth, elevation and transmission.

Separate but closely spaced transducer pairs were used for transmission and reception of acoustic signals. Three transmit/receive combinations were used, corresponding to centre frequencies of 34 kHz, 100 kHz and 204 kHz. The 34 kHz and the 100 kHz transducers were internally tuned and could be coupled directly to the output stage. The 204 kHz transducer required an external tuning circuit. The transmit signals were unshaded FM pulses of 1 msec duration, with chirp bandwidths of 5 kHz at 34 kHz and 204 kHz, and 3 kHz at 100 kHz.

While all transducers could be simultaneously mounted on the structure only two channels were available for acoustic data and not all frequencies could be surveyed at each deployment. Since the 204 kHz transducer was externally tuned it was left permanently connected. The 34 kHz and 100 kHz transducers were connected as required.

The bottom reverberation data were band passed and low pass filtered at 20 kHz prior to analogue-to-digital conversion at 100 kHz. Digitized data records were stored to write-once-read-many (WORM) disks, together with system control log files and calibration data. At each elevation angle and for each transmission frequency returns from 50 pings were logged. Each sequence of 50 pings took about 30 seconds to acquire.

Calibration of the acoustic system was performed with transmit and receive transducers facing each other and separated by approximately 2.3 metres. Calibration data was logged with the same hardware and procedures as for bottom backscatter data. In this manner, calibration included all system elements.

4. Experiments

Summaries of experiment deployments are shown in the experiment data summary, shown in table 1, which includes details of deployment, date and location.

4.1 Experiment Procedure

At most sites measurements were made at five different azimuths separated by 45°, i.e. at azimuths of -80°, -35°, +10°, +55° and +100°, measured relative to the +X direction of the tower co-ordinate system. The beam angle was varied by tilting the transducer array between 2.5° and 50° from horizontal. At shallow angles between 2.5° and 15° the tilt angle was incremented in 2.5° steps. Above 15° the interval was 5°. The actual transmit beam angle was calculated from the transducer tilt and the structure inclination. Where time permitted additional sequences using CW transmissions were conducted although these were restricted to azimuth 10°.

At most stations azimuth sweeps from -85° to +145° in 15° steps at a constant beam elevation of 10° were also performed.

Variable depth sonars typically operate between 30 and 40 kHz in detection mode, while for contact classification frequencies greater than 200 kHz are commonly used. For these reasons measurements at 34 kHz and 204 kHz were considered higher priority than at 100 kHz, and were conducted during the one deployment. Where time and conditions permitted data at 100 kHz were obtained by recovering the equipment, swapping the 34 kHz and 100 kHz connections and redeploying.

Table 1: Experiment Data Summary Sheet.

Deployment No.	Task	Site	Date	Time	Latitude	Longitude	Depth (m)	Sound Speed	Temp
37	Cal.	Darwin	2 Mar				10	1540.0	28.8
38	BBS	N1	4 Mar	11:55	12° 03.65S	130° 41.80E	28	1543.0	28.8
39	BBS	N2	5 Mar	12:55	12° 03.03S	130° 41.93E	*	1543.0	28.8
40	BBS	N2	5 Mar	20:00	12° 03.03S	130° 41.93E	*	1543.0	28.8
41	BBS	N3	6 Mar	13:25	12° 01.84S	130° 42.85E	28	1543.6	28.9
42	BBS	N3	7 Mar	09:00	12° 01.88S	130° 42.86E	29	1544.0	29.1
43	BBS	N3	7 Mar	10:25	12° 01.88S	130° 42.86E	28	1544.0	29.1
44	BBS	N4	7 Mar	14:15	12° 01.45S	130° 41.18E	29	1544.4	29.2
45	BBS	N4	7 Mar	16:15	12° 01.45S	130° 41.18E	29	1544.4	29.2
46	BBS	W1	8 Mar	08:05	12° 15.12S	130° 08.75E	38	1544.4	29.2
47	BBS	W1	8 Mar	14:00	12° 15.20S	130° 08.87E	38	1544.4	29.2
48	BBS	W2	9 Mar	08:10	12° 15.94S	130° 08.92E	39	1544.4	29.2
49	BBS	W2	9 Mar	14:40	12° 15.94S	130° 08.92E	39	1544.4	29.2
50	BBS	W3	10 Mar	10:10	12° 16.90S	130° 09.18E	37	1544.6	29.3
51	BBS	W3	10 Mar	16:00	12° 16.94S	130° 08.28E	37	1544.4	29.2
52	BBS	W4	11 Mar	09:50	12° 17.81S	130° 07.53E	38	1544.4	29.2
53	Cal.	En route	11 Mar	15:45					

(* no data was obtained at N2 due to equipment failure)

4.2 Data Analysis

At steep ray angles and short ranges the effects of refraction and ray bending on transmission paths are negligible and can be ignored. However if the sound speed profile is not isovelocity then at the low grazing angles and correspondingly long ranges which are of most interest here, the sound speed profile can significantly influence the ray geometry and its effects should not be ignored. Refraction effects are manifest in two ways. First, as a result of ray bending, the bottom grazing angle will generally be different from the launch angle at the transducer array. Second, as a consequence of beam convergence or divergence, the area insonified will be distorted compared to spherical spreading. Since the backscatter is the product of the backscattering strength and the area insonified the area needs to be reliably estimated in order to determine the backscattering strength.

A simple ray tracing program was used to model propagation paths between the transducer array and the bottom; and to relate launch angle, bottom grazing angle, horizontal range, path length and travel time. The water column was assumed to be horizontally stratified, with the sound speed profile as measured at the time of the experiment.

For each ping the mean level of the backscatter return was calculated by taking the RMS average of data points corresponding to a narrow spread of angles centred about the beam elevation angle. This angular aperture varied with the secant of the elevation angle from $\pm 1^\circ$ at 60° elevation, to $\pm 0.5^\circ$ at 2.5° elevation.

The linear average and standard deviation of the RMS values were computed from the 50 pings. Pings whose average level was more than 3 standard deviations from the mean were rejected from the data set. The mean of the filtered data set was recalculated to give the average bottom return.

The bottom backscattering strength S_b in dB was calculated from the equation

$$S_b = RL - SL + 40\log r + 2\alpha r + 20\log C_s - 10\log A$$

where SL is source level, RL is the reverberation level, r is range in metres, α is the absorption coefficient (dB/m), C_s is a correction factor for ray divergence or convergence [2] and A is the area of the sea bottom insonified (m^2). The beam spreading correction factor C_s represents the ratio of the actual area insonified under the influence of the measured sound speed profile to the ideal insonified area assuming straight line propagation and spherical spreading in an isovelocity medium.

The absorption coefficient α was calculated from the Francois-Garrison equation [9].

The area of the bottom insonified by the acoustic transmission depends on the transducer beam pattern, the length of the acoustic pulse, the grazing angle and the range. The beam patterns of the transducers were circularly symmetric and the insonified area of the bottom was taken as the projection on the bottom of the transmit beam at the -3 dB points of the beam. Unless the grazing angle is steep the radial extent of the insonified area is limited by the pulse length, while the width depends on the array (horizontal) beamwidth. The insonified area was given by

$$A = r\beta \left(\frac{c\tau}{2} \right) \sec \theta_g$$

where β is the beamwidth of the transducer array, c is the sound speed, τ the pulse length and θ_g is the grazing angle.

Directional transducers were used for transmit and receive. The effective beamwidth β_{array} of the combined projector and hydrophone array was calculated from the -3 dB beamwidths of the projector β_{proj} and hydrophone β_{hp} by the formula [2]

$$\beta_{array} = 1.065 \left(\beta_{hp}^{-2} + \beta_{proj}^{-2} \right)^{-\frac{1}{2}}$$

If the transmit and receive beam patterns are identical, as was the case for this experiment, $\beta_{hp} = \beta_{proj} = \beta$, and the array beamwidth $\beta_{array} = 0.7532\beta$. For the transducer pairs used the resultant array beamwidths were 12° at 34 kHz, 11° at 100 kHz and 6° at 204 kHz.

5. Results

The data were analysed to determine the dependence of bottom backscattering strength on grazing angle, azimuth, transmit frequency and, as several different sites were occupied, bottom type. In all eight sites, four in area 207 and four in area 214, were investigated. Due to time and tidal constraints it was not possible to conduct measurements at all sites at all frequencies. Measurements at 34 kHz and 204 kHz were conducted at 7 sites while data at 100 kHz was collected at 3 sites only. No data was recorded at N2 due to equipment malfunction. Table 2 shows measurements conducted at sites occupied.

Table 2. Site measurement matrix.

Site	34 kHz	100 kHz	204 kHz
N1	✓	✗	✓
N2	✗	✗	✗
N3	✓	✓	✓
N4	✓	✗	✓
W1	✓	✓	✓
W2	✓	✗	✓
W3	✓	✓	✓
W4	✓	✗	✓

5.1 Variation of bottom backscattering strength with grazing angle.

At most sites, and for each frequency, measurements were conducted using FM transmissions at five different azimuths spanning -80° to +100°. The azimuth sequence was not always the same order, but the pan angles were always spaced at

45° intervals. Where time permitted additional measurements at azimuth +10° with CW transmissions were made.

The transducer beam patterns were too narrow to facilitate measurements over a wide spread of grazing angles at a single array elevation. Close to the array axis the beam response was sensibly uniform but it dropped rapidly as the angle off axis increased. By restricting the measurements to a small angular spread close to the transducer axis the effects of the beam pattern could be ignored. The worst case situation occurred with the 204 kHz transducers which had the narrowest beam pattern, but even in this instance the array response at 1.5° from the beam axis was within 0.3 dB of the maximum.

For each transmit beam angle the bottom backscattering strengths measured along the beam axis and additionally at $\pm 1^\circ$ from the axis were calculated. The measurements at $\pm 1^\circ$ conveniently fell in between the 2.5° array elevation angle increments at the shallowest angles, and since the insonified areas did not overlap, these estimates were independent. Three estimates of backscattering strength were thus obtained at each array elevation.

The minimum array elevation angle was 2.5° and, as data at one degree above and below the beam axis were also analysed, backscattering strengths down to approximately 1.5° grazing were potentially available. In practice this limit was not achieved. In negative sound speed gradients downward refraction generally restricted the minimum grazing angle to more than 2°. In positive sound speed gradients rays were refracted upwards so that returns from the shallowest grazing angles were sometimes outside the time window of the sampled data.

Two other areas for potential data corruption existed. First, as the grazing angle decreased, the sensitivity of the calculations to uncertainties in raypaths and transmission loss increased to the point where the uncertainty was sufficient to make the backscattering strength estimates unreliable. Second, contamination by surface backscattering at grazing angles below about 3° in water depths up to 18m has been identified by Boeheme *et al.* [1, 2]. This interference appears to arrive via direct and bottom reflected paths and can be significant if the sea surface is rough. Its influence is apparent as a jump in backscattering strength as the grazing angle decreases. Some of the data measured in this experiment showed similar characteristics, but it has been included for completeness. A third possibility for data contamination exists in that, at the shallowest grazing angles when acoustic returns are lowest and the system gains are highest, the data may be system noise limited.

Results from the backscatter measurements are presented in graphical format in Figures 3 to 19. The top graph in each figure shows variation in backscattering strength with actual grazing angle as calculated by ray tracing. Generally there are five and frequently six data sets, corresponding to the range of azimuths. The different symbols on the graphs represent data measured at different azimuth angles.

At the steepest grazing angles measured, backscattering strengths were characteristically between -20 dB and -30 dB. As the grazing angle reduced the backscattering strength decreased so that at the shallowest elevations it was typically between -40 dB and -50 dB.

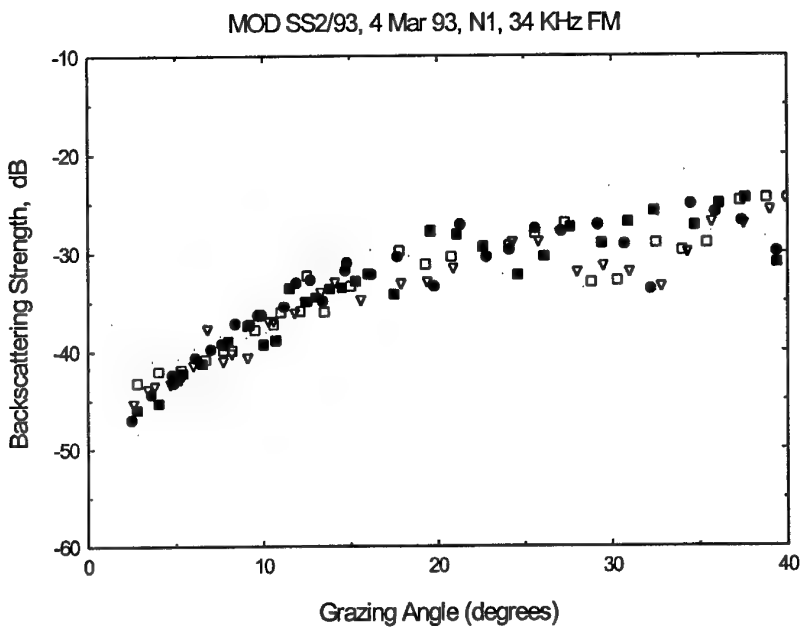


Figure 3A Bottom backscattering strength at 34 kHz, site N1, area 207.
Relative azimuths -80°, -35°, 10°, 55° and 100°.

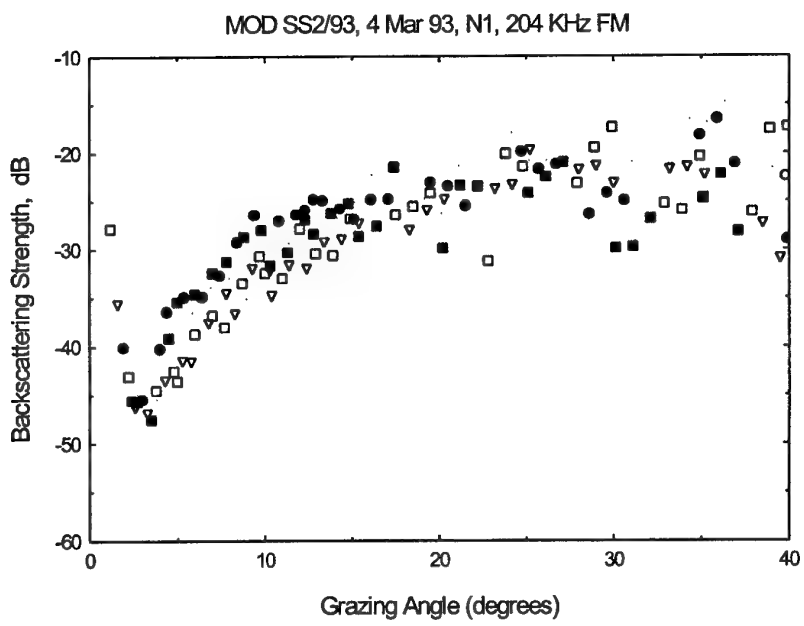


Figure 3B Bottom backscattering strength at 204 kHz, site N1, area 207.
Relative azimuths -80°, -35°, 10°, 55° and 100°.

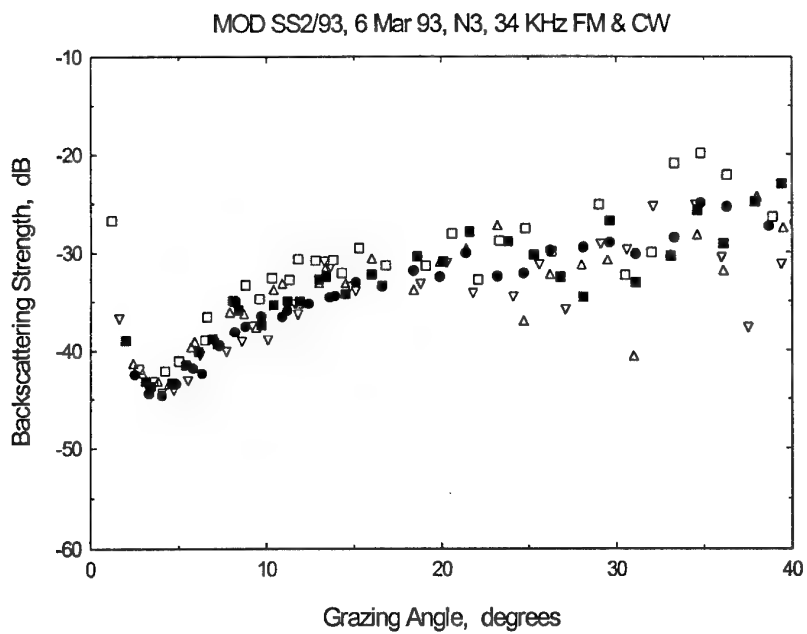


Figure 4A Bottom backscattering strength at 34 kHz, site N3, area 207.

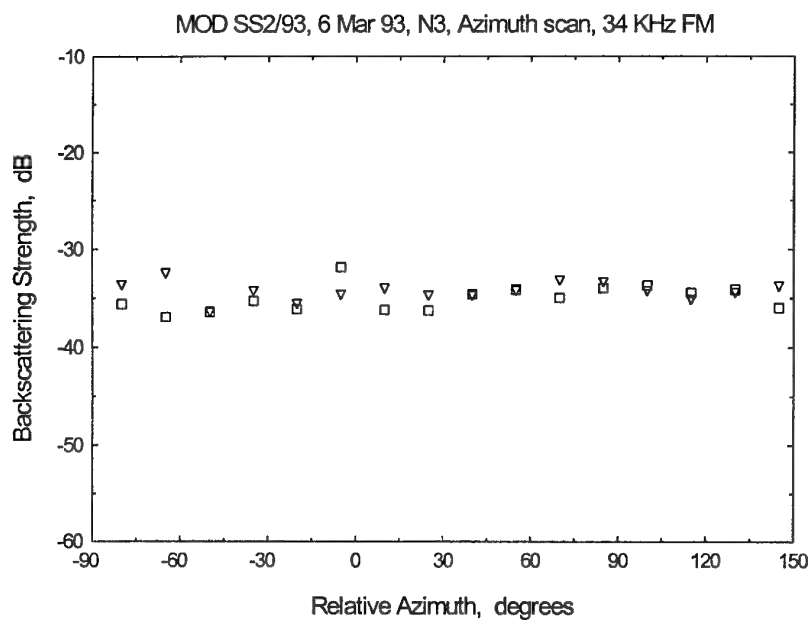


Figure 4B Bottom backscattering strength at 34 kHz, azimuth scan, site N3, area 207.

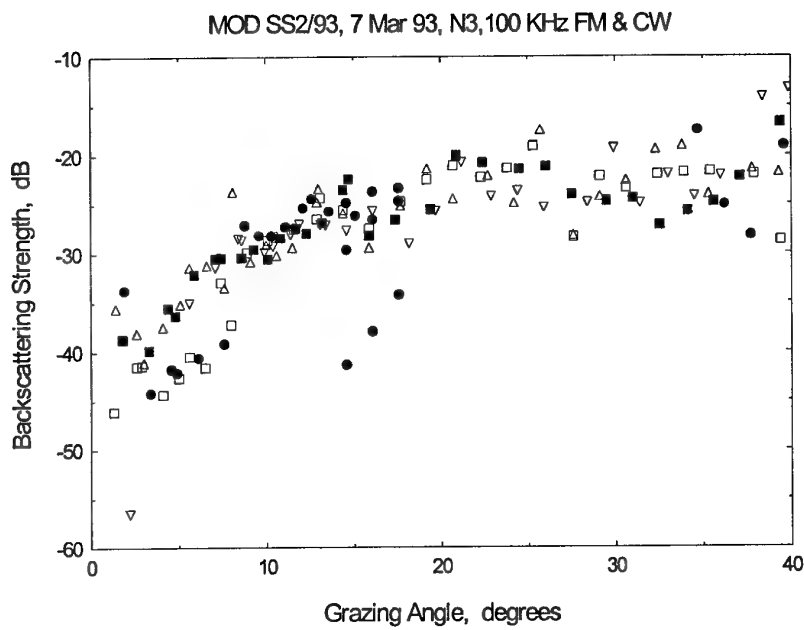


Figure 4C Bottom backscattering strength at 100 kHz, site N3, area 207.

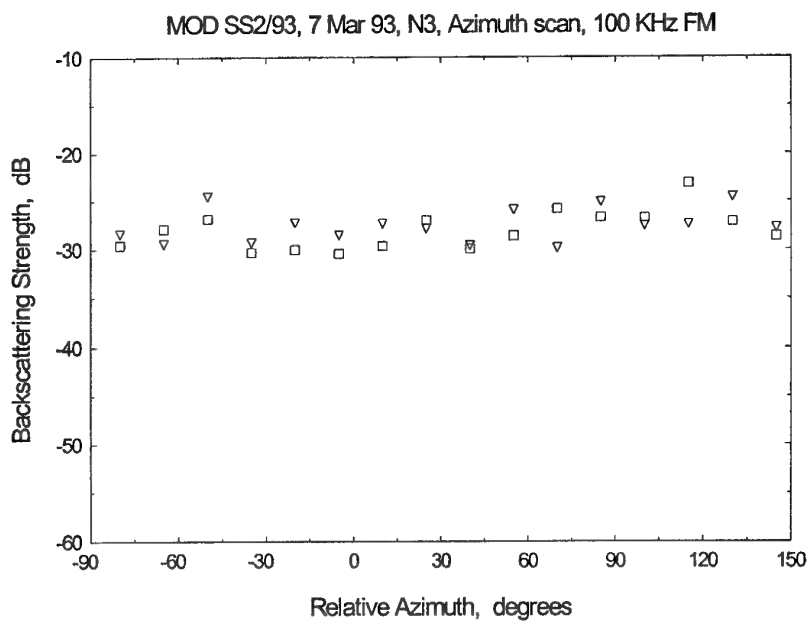


Figure 4D Bottom backscattering strength at 100 kHz, azimuth scan, site N3, area 207.

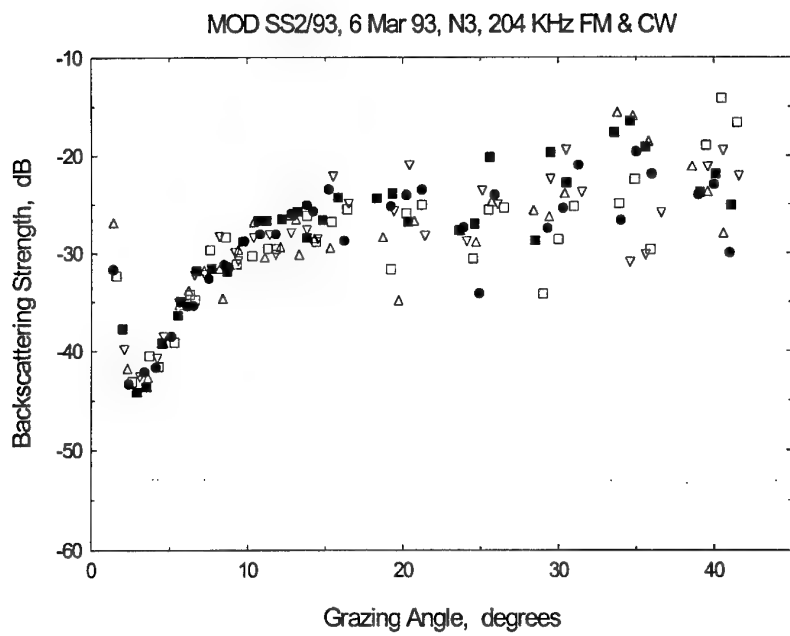


Figure 4E. Bottom backscattering strength at 204 kHz, site N4, area 207.

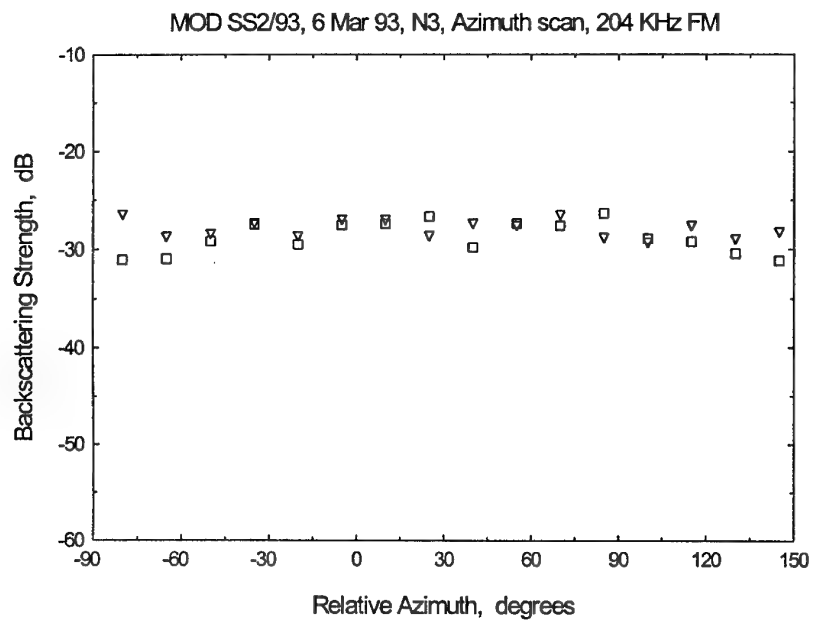


Figure 4F. Bottom backscattering strength at 204 kHz, azimuth scan, site N4, area 207.

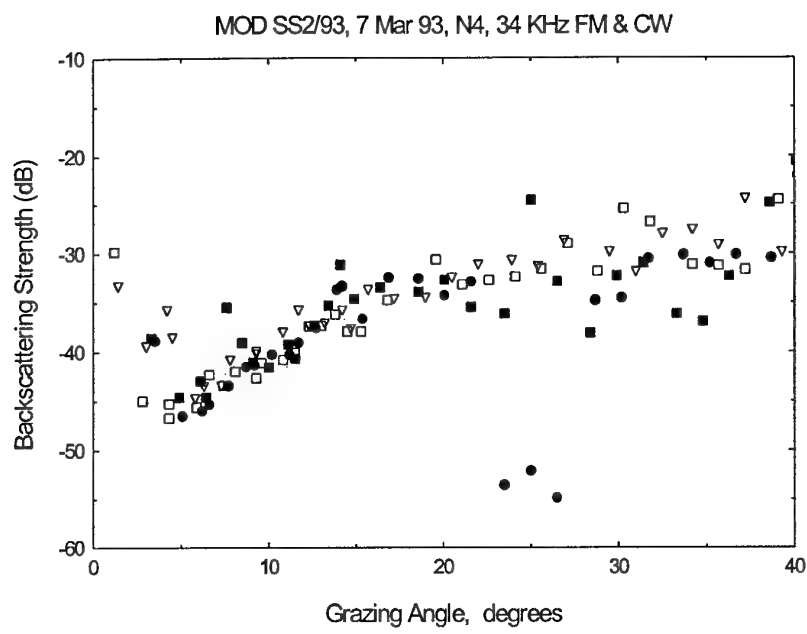


Figure 5A Bottom backscattering strength at 34 kHz, site N4, area 207.

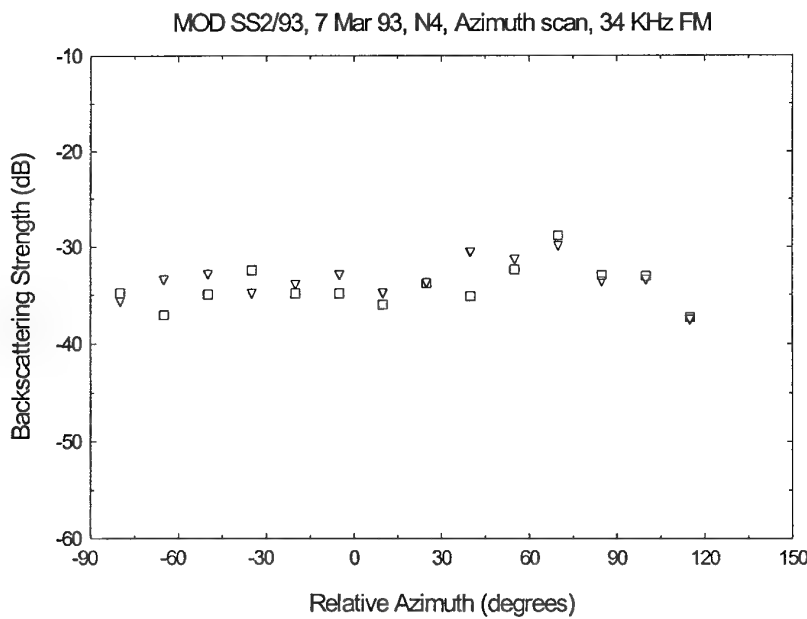


Figure 5B Bottom backscattering strength at 34 kHz, azimuth scan, site N4, area 207.

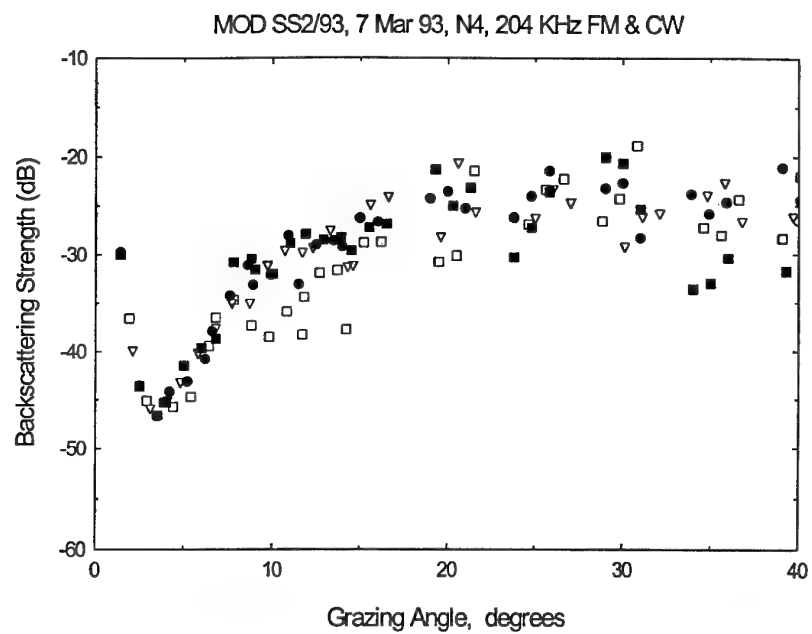


Figure 5C. Bottom backscattering strength at 204 kHz, site N4, area 207.

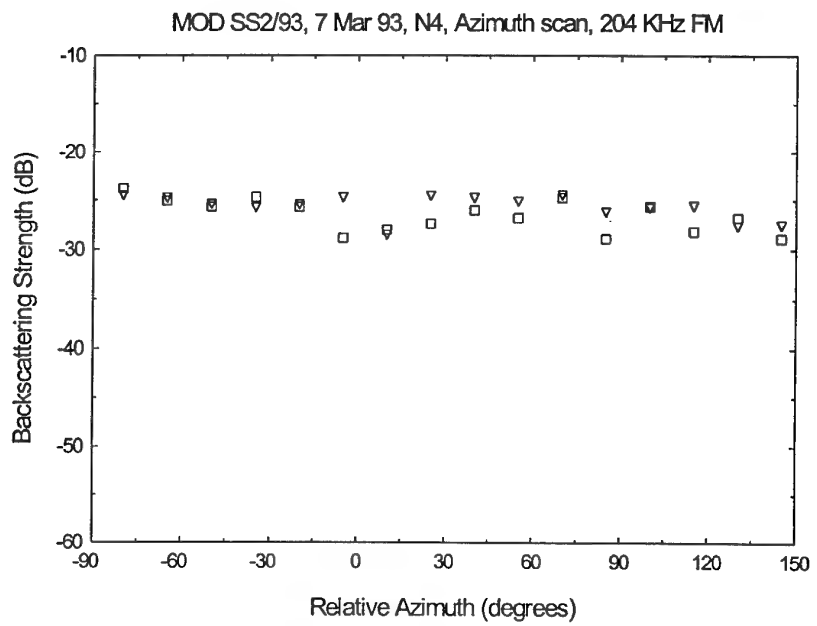


Figure 5D. Bottom backscattering strength at 204 kHz, azimuth scan, site N4, area 207.

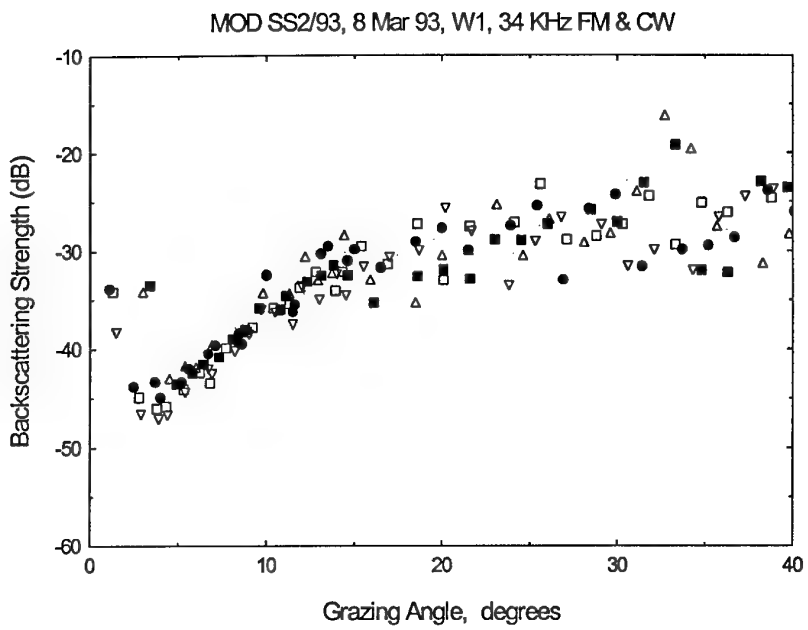


Figure 6A. Bottom backscattering strength at 34 kHz, site W1, area 214.

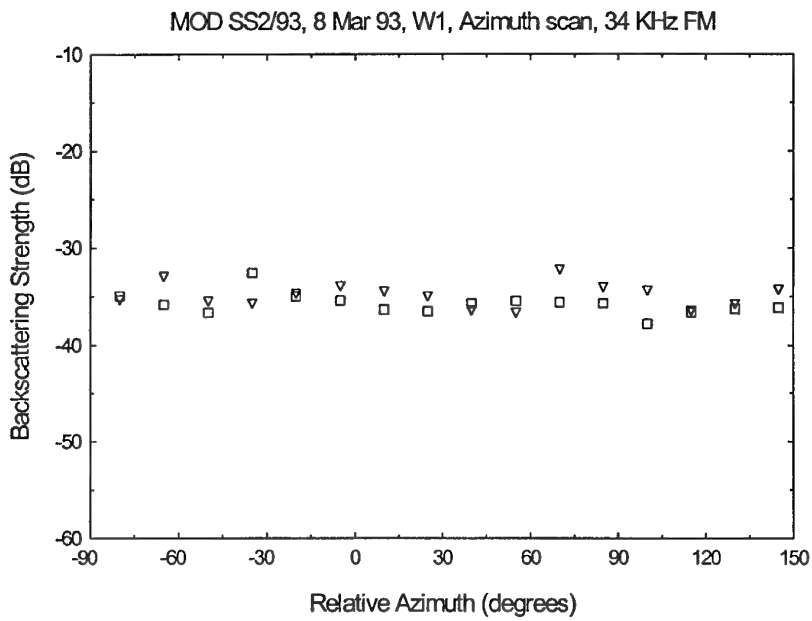


Figure 6B. Bottom backscattering strength at 34 kHz, azimuth scan, site W1, area 214.

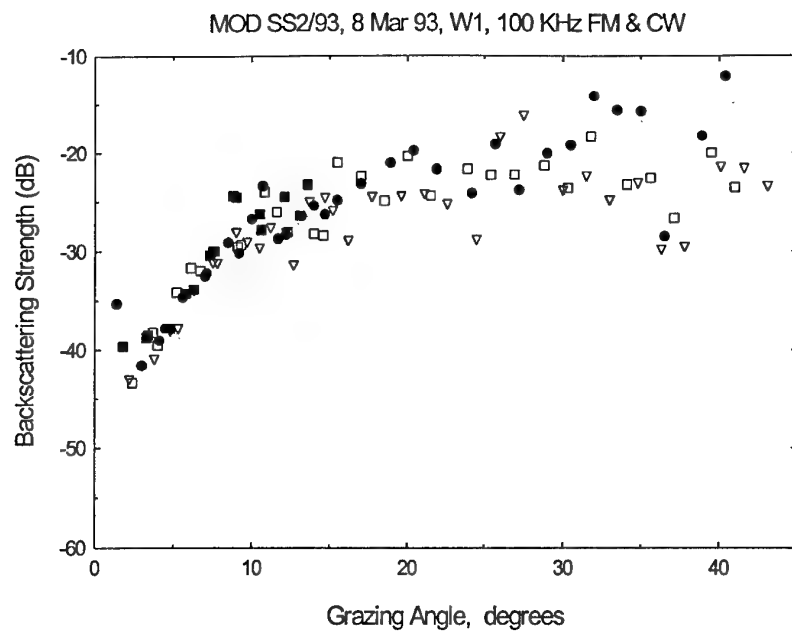


Figure 6C. Bottom backscattering strength at 100 kHz, site W1, area 214.

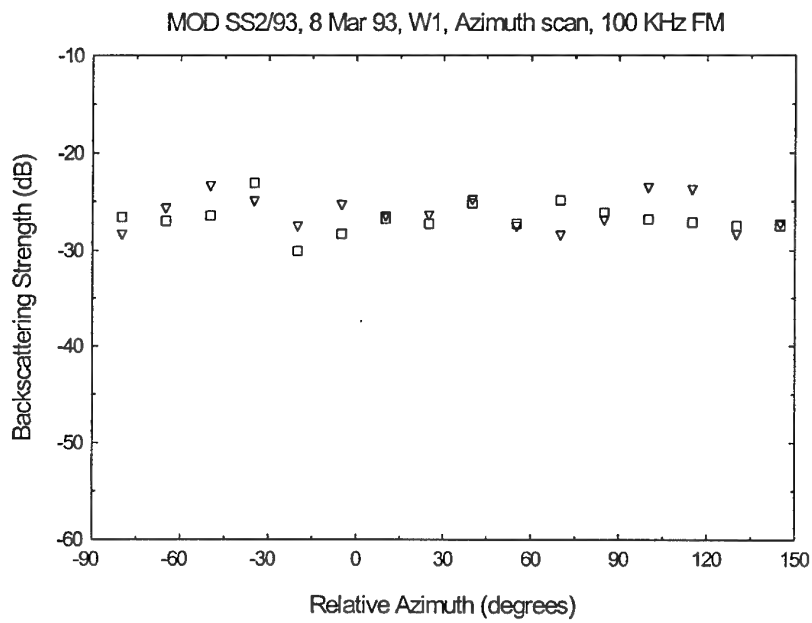


Figure 6D. Bottom backscattering strength at 100 kHz, azimuth scan, site W1, area 214.

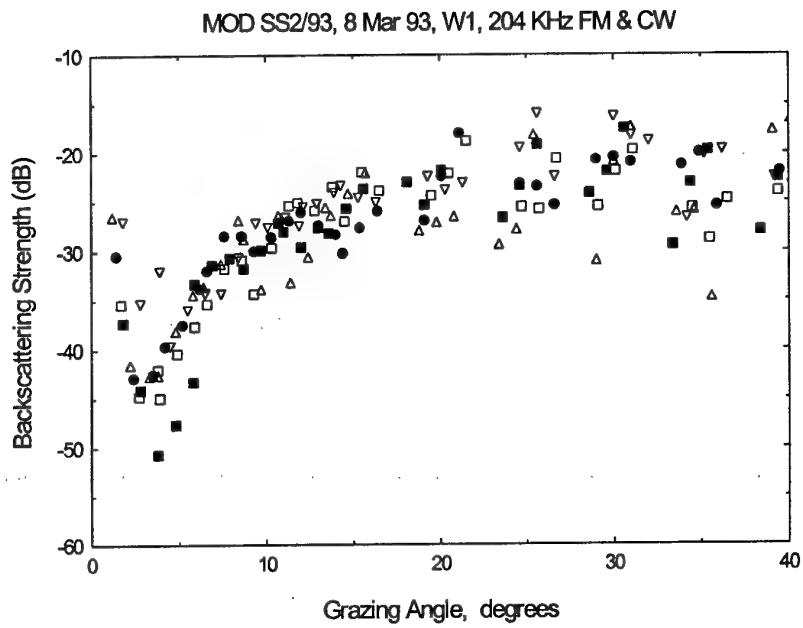


Figure 6E. Bottom backscattering strength at 204 kHz, site W1, area 214.

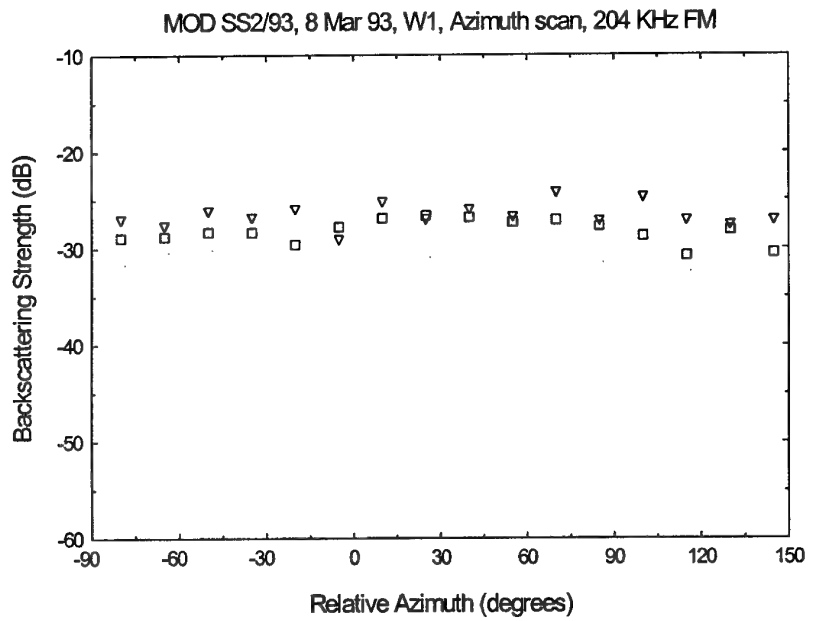


Figure 6F. Bottom backscattering strength at 204 kHz, azimuth scan, site W1, area 214.

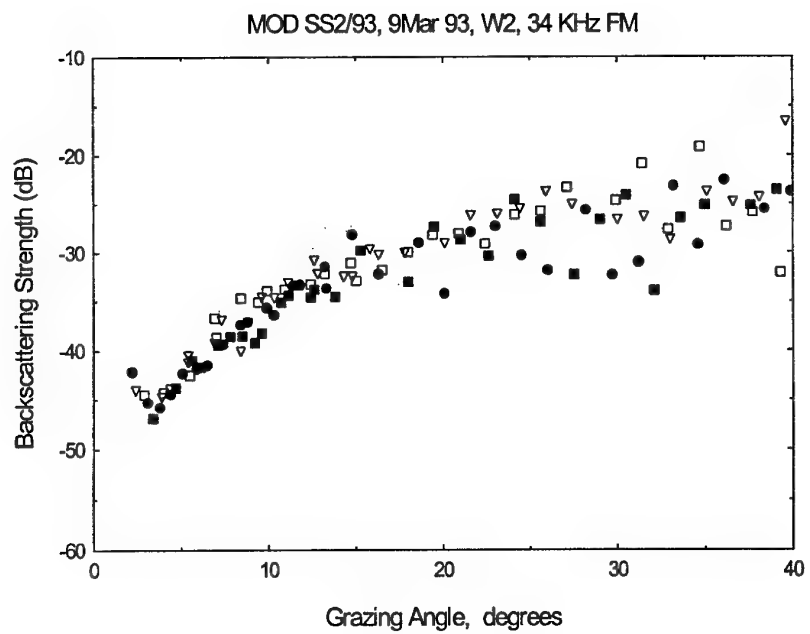


Figure 7A. Bottom backscattering strength at 34 kHz, site W2, area 214.

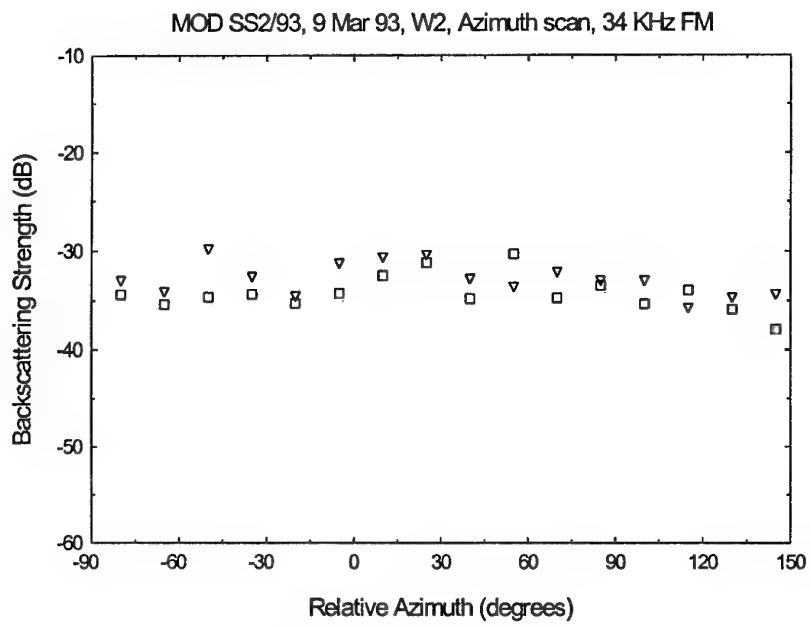


Figure 7B. Bottom backscattering strength at 34 kHz, azimuth scan, site W2, area 214.

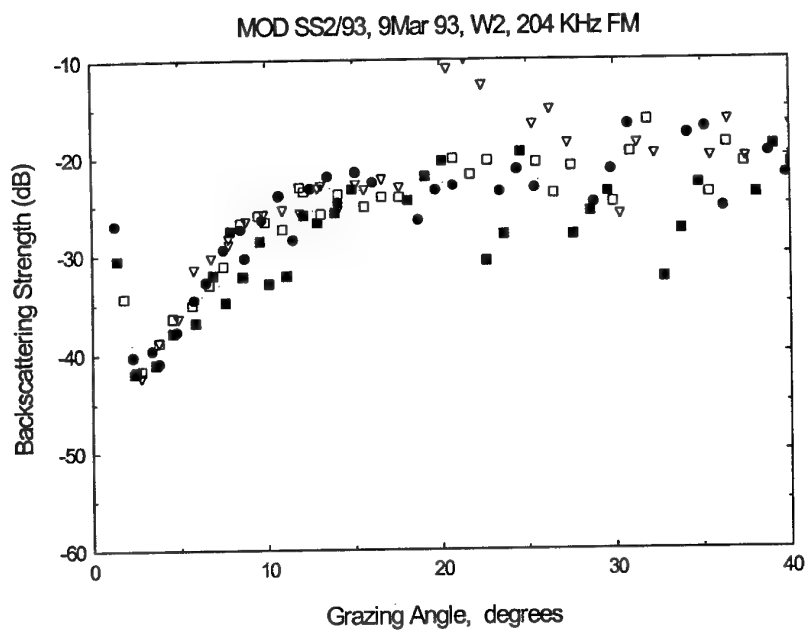


Figure 7C. Bottom backscattering strength at 204 kHz, site W2, area 214.

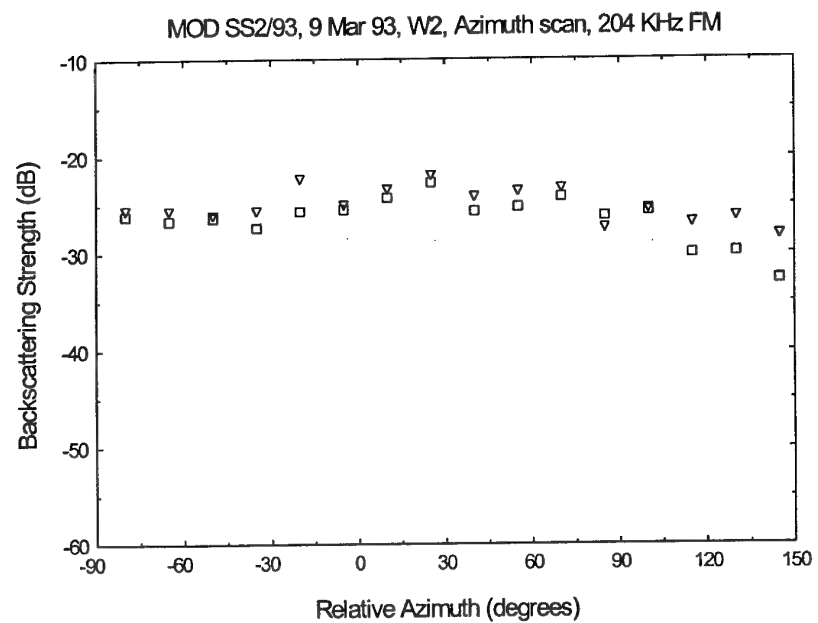


Figure 7D. Bottom backscattering strength at 204 kHz, azimuth scan, site W2, area 214.

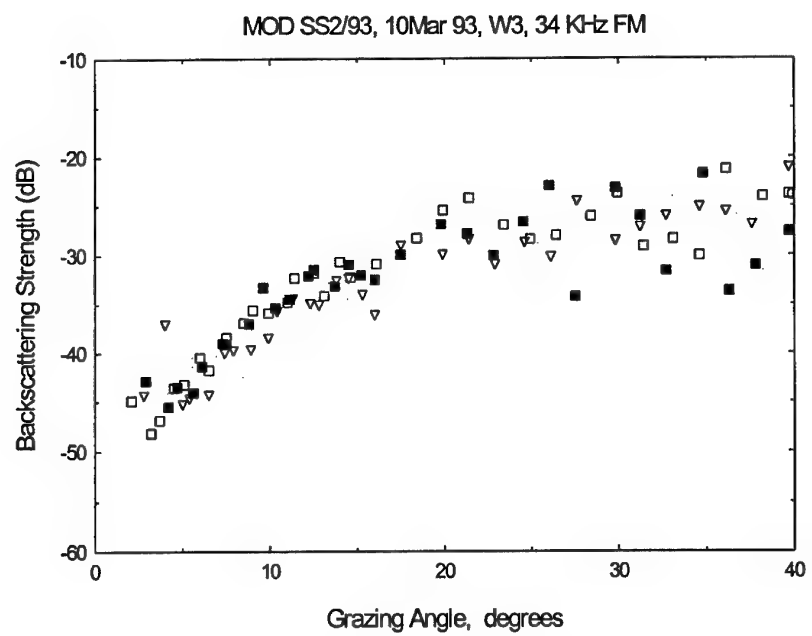


Figure 8A. Bottom backscattering strength at 34 kHz, site W3, area 214.

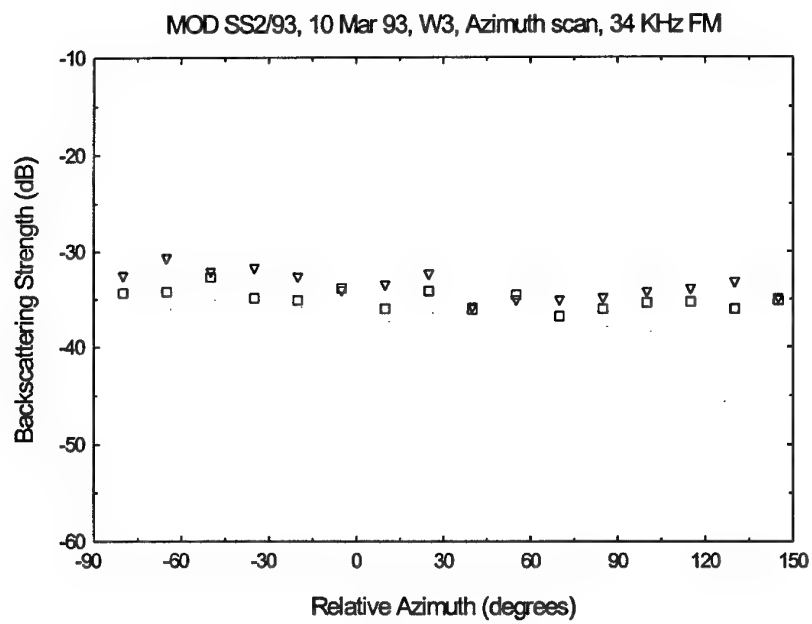


Figure 8B. Bottom backscattering strength at 34 kHz, azimuth scan, site W3, area 214.

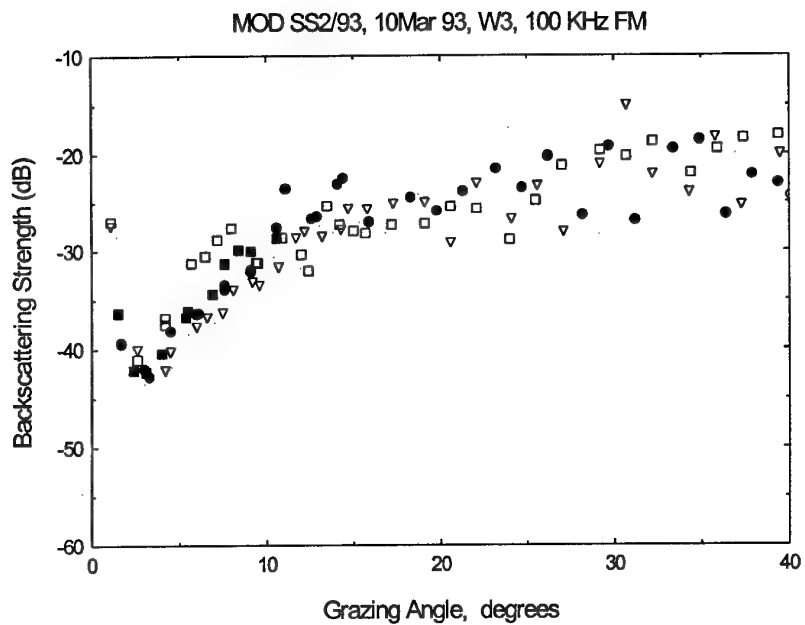


Figure 8C. Bottom backscattering strength at 100 kHz, site W3, area 214.

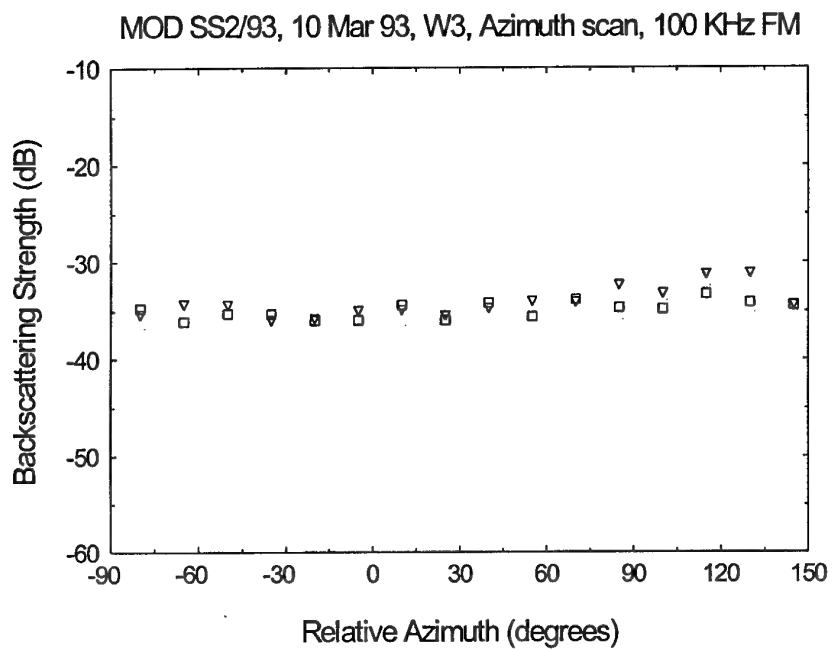


Figure 8D. Bottom backscattering strength at 100 kHz, azimuth scan, site W3, area 214.

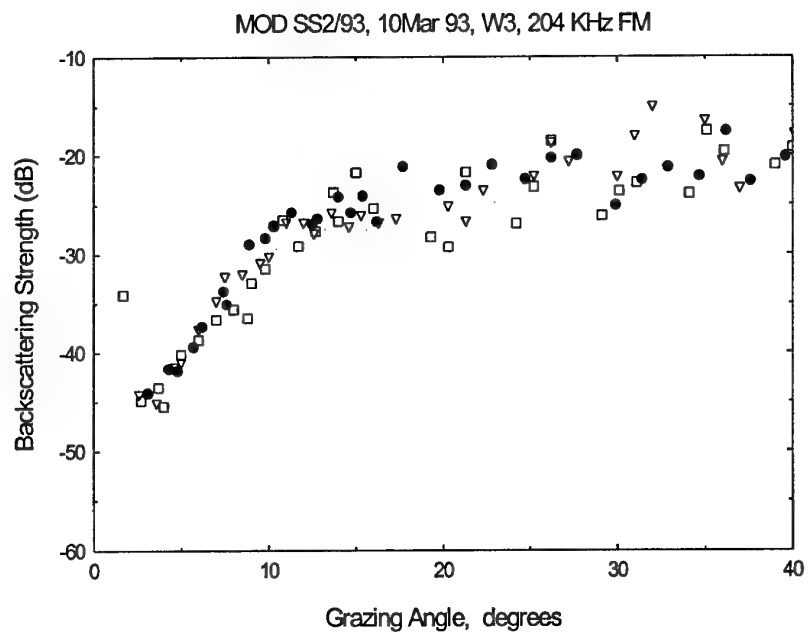


Figure 8E. Bottom backscattering strength at 204 kHz, site W3, area 214.

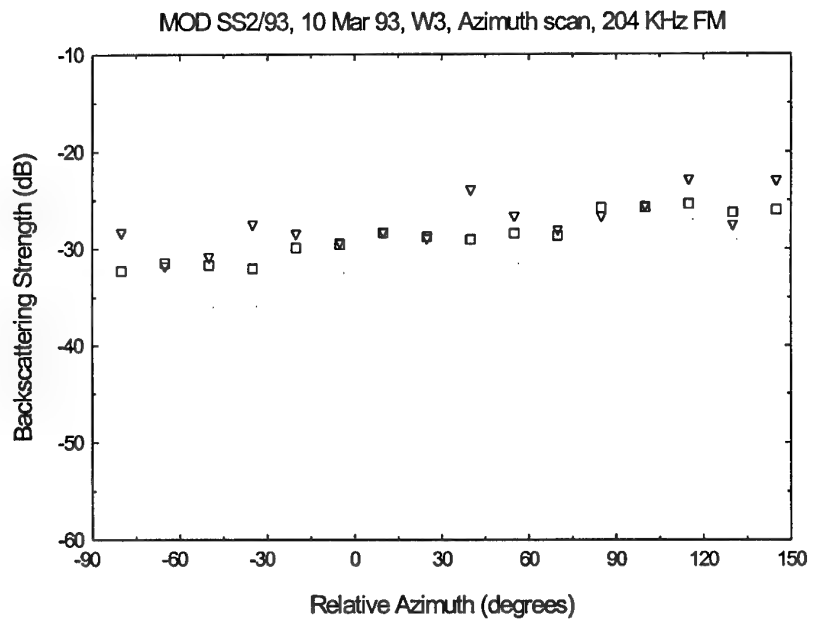


Figure 8F. Bottom backscattering strength at 204 kHz, azimuth scan, site W3, area 214.

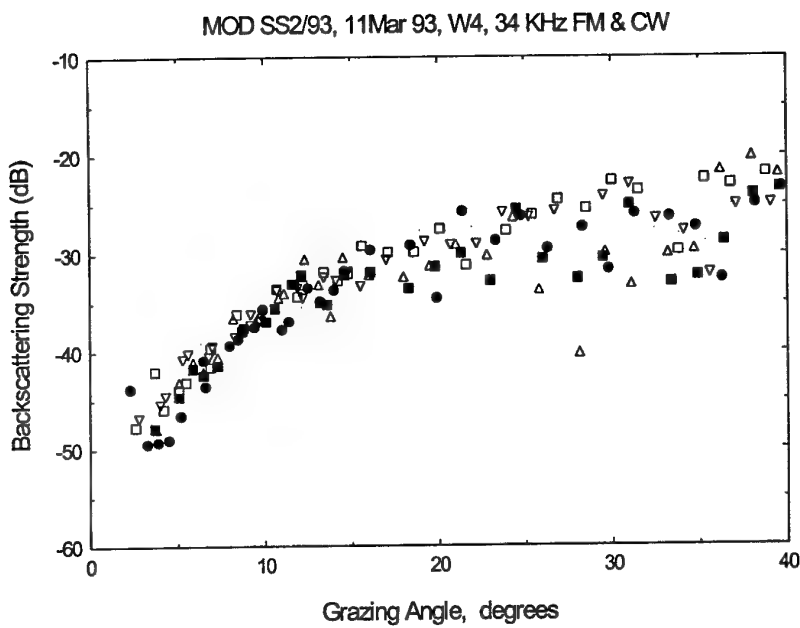


Figure 9A. Bottom backscattering strength at 34 kHz, site W4, area 214.

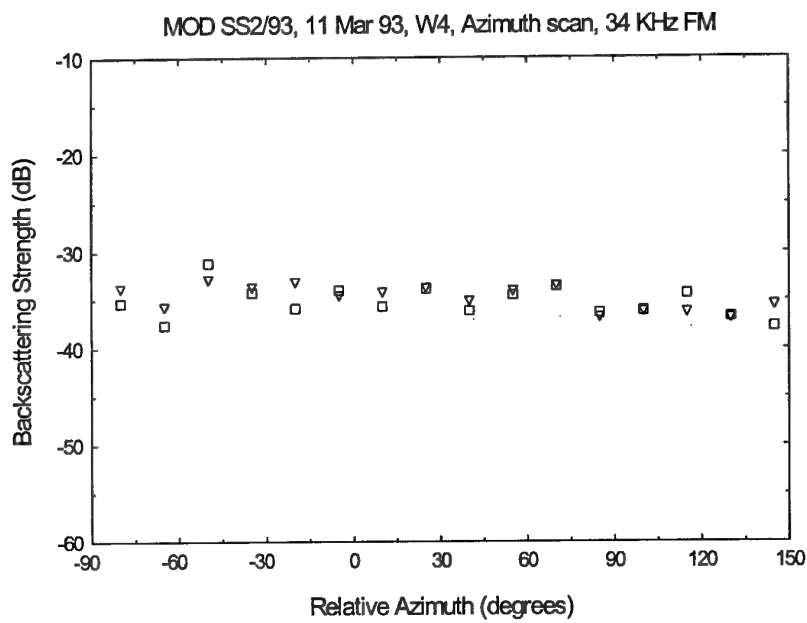


Figure 9B. Bottom backscattering strength at 34 kHz, azimuth scan, site W4, area 214.

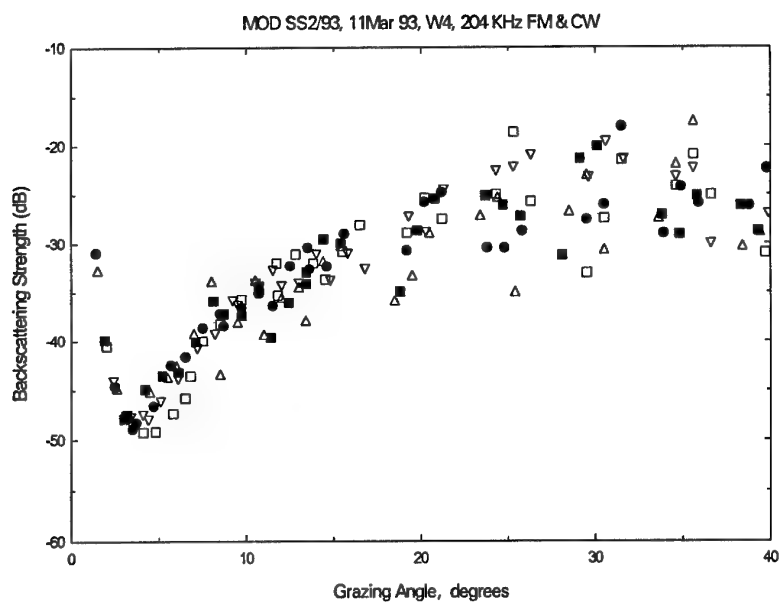


Figure 9C. Bottom backscattering strength at 204 kHz, site W4, area 214.

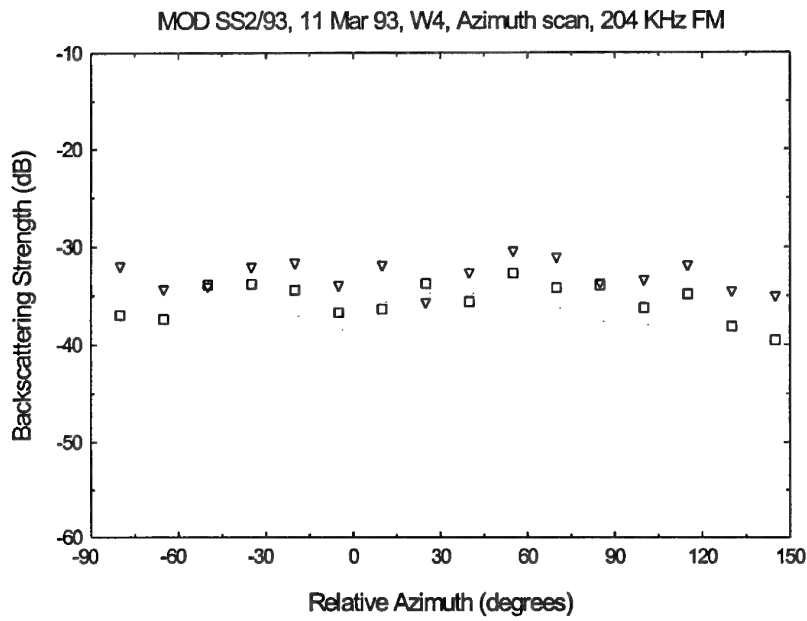


Figure 9D. Bottom backscattering strength at 204 kHz, azimuth scan, site W4, area 214.

5.2 Frequency Dependence

Several papers have investigated the frequency dependence of backscattering strength at grazing angles near 10° over sandy bottoms, and a range of dependencies has been reported. In some of the earliest measurements published, McKinney and Anderson [2] found frequency dependence slightly less than 5 dB per octave. In more recent studies weaker dependencies have been reported. Jackson *et al* [5] in a series of experiments in UK and US waters measured slopes between 1 and 2 dB/octave over medium and fine sandy bottoms. Boehme *et al* [3] determined frequency dependencies between 3 and 4.5 dB/oct over a sand bottom near San Diego, California.

The data reported here show that, for grazing angles near 10°, at most sites the backscattering at 204 kHz was higher than that at 34 kHz by about 6 to 8 dB, although the difference tended to reduce as the grazing angle decreased. The exception was at W4 where the scattering strength at 204 kHz was about 6 dB lower than at the other six sites, and little different from the backscattering strength at 34 kHz. At site N4 scattering strengths at both 34 kHz and 204 kHz were lower than at other sites by about 3 dB, but the difference between the frequencies was maintained.

If the data from site W4 is disregarded, these results suggest scattering strengths increasing at between 2.4 and 3.2 dB/oct in both areas.

Measurements were made at 100 kHz only at sites N3, W1 and W3. These data approximate the measurements at 204 kHz at the same sites.

5.3 Variation with Azimuth.

At most stations azimuth sweeps from -85° to +145° in 15° steps were also performed. These measurements were intended to identify any azimuthal dependence or anisotropy in backscattering strength. Since the experiment sites had been selected by side scan survey to be fairly uniform and clear of irregularities little azimuthal dependence was anticipated.

For these measurements the array tilt angle was maintained constant at 10°. At most sites the tower structure did not sit exactly horizontal on the bottom but was tilted slightly. Consequently the transducer tilt angle, which was measured relative to the tower co-ordinate system, differed slightly from the actual beam depression angle, which was measured relative to the world co-ordinate system. The beam launch angle varied about the 10° angle of the transducer tilt by an amount which depended on the tower inclination, orientation and the beam azimuth. In practice the actual bottom grazing angle differed from the transducer tilt by up to 1.5°, and the difference in bottom grazing angles across the scan frequently exceeded 2°.

Where included the lower graph in each figure shows the dependence of bottom backscattering on azimuth for the array tilt angle of 10°. Because of the variation in beam launch angle with azimuth there is embedded in these curves a slight grazing angle dependence which complicates the pattern of azimuthal dependence. These curves are intended to show gross dependencies rather than fine detail. The data from the azimuth scans are consistent with the elevation data. That is there is a few

dB spread in backscattering strength measured at different azimuths but no consistent dependence on bearing. No data to date has shown strong azimuthal dependence.

5.4 Bottom Characterization

It is generally agreed that high frequency acoustic energy is scattered and reflected from the upper few centimetres of the sea floor sediment and that the bottom backscattering strength depends on the composition of this near surface material and on the surface roughness, although the mechanisms of the physical processes are not fully understood.

Generally backscattering strength increases with increasing sediment grain size. Low backscattering strengths tend to be associated with fine soft silty sediments, while coarse hard sediments yield backscattering strengths several decibels higher. Sediment grain size and sediment composition is thus a useful and important parameter in characterising the bottom back scattering strength of the sea floor sediment.

To complement the acoustic data analysis bottom grab samples and stereo photographs were obtained at each site. During the experiments bottom samples were obtained by a grab sampler. At that time visual observations estimated the sediments in both areas to be predominantly fine to medium sand having a particle size 0.125-0.5 mm diameter corresponding to phi values between 1 and 3, with traces of finer silty components. Bottom photography showed some evidence of bio-turbidation, but little surface relief or vegetation. At no site were well defined sand ripples observed.

At most sites in Area 207 small shell fragments up to 12 mm were evident in the samples and also in the bottom photographs. In Area 214 fewer shells were observed but small pebbles were also present. Post cruise, the proportions of gravel, sand and mud in each sample were determined by wet sieving through 2 mm and 63 mm analytical sieves. Sediment compositions are shown in table 3.

Table 3 . Sediment classification, SS2/93.

Site	Deployment	%Mud	%Sand	%Gravel	Density gm/cc	Porosity
N1	38	6.2	80.7	13.0	2.615	0.473
N1	38	4.8	75.3	19.9	2.641	0.497
N2	39	18.3	66.9	14.8	2.485	0.487
N2	39	12.0	71.8	16.2	2.615	0.525
N3	41	8.5	77.8	13.7	2.591	0.543
N3	41	15.0	77.9	7.1	2.525	0.502
N4	44	9.2	75.2	15.6	2.589	0.470
W1	45	5.1	70.3	24.6	2.639	0.416
W1	47	8.0	85.4	6.6	2.619	0.468
W2	48	9.8	76.6	13.6	2.522	0.458
W2	49	11.7	71.8	16.5	2.607	0.474
W3	50	10.5	76.0	13.5	2.634	0.448
W3	50	11.3	78.8	9.9	2.602	0.438
W4	52	16.0	80.4	3.6	2.597	0.458

6. Conclusion

Bottom backscattering strengths in the Darwin area have been measured at 34 kHz, 100 kHz and 204 kHz for a range of grazing angles from approximately 2° to 40°. The lower angular limit was set by interfering surface reverberation and uncertainty in the transmission paths at shallow grazing angles.

The results are consistent with reported data for similar bottom types and show a rapid decrease in bottom backscattering strength as the grazing angle decreases below 10°. The steepest grazing angle in the experiments was 40°, so it was not possible to determine the rapid increase in backscattering strength as the grazing angle approaches 90° which has been reported by Jackson *et al.* [5].

No significant anisotropy was observed for grazing angles near 10°. This is consistent with the lack of observed sand ripples in bottom photographs.

At all but one site backscattering strength increased with frequency by about 2 to 3 dB per octave. This frequency dependence is in the midrange of rates reported in the open literature for similar bottom types.

7. References

1. *APL-UW High Frequency Ocean Environment Acoustic Models (I)*. Technical Report APL_UW TR8907, November 1989.
2. C.M. McKinney and C.D. Anderson (1964) *Measurements of Backscattering of Sound from the Ocean Bottom*. J. Acoust. Soc. Am., **36** 158-163.
3. H. Boehme, N.P. Chotiros, L.D. Rolleigh, S.P. Pitt, A.L. Garcia, T.G. Goldsberry and R.A. Lamb (1985) *Acoustic backscattering at low grazing angles from the ocean bottom. Part I. Bottom backscattering strength*. J. Acoust. Soc. Am., **77**, 962-974.
4. H. Boehme and N.P. Chotiros (1988) *Acoustic backscattering at low grazing angles from the ocean bottom*. J. Acoust. Soc. Am., **84**, 1018-1029.
5. D.R. Jackson, A.M. Baird, J.J. Crisp and P.A.G. Thomson (1986) *High-frequency bottom backscatter measurements in shallow water*. J. Acoust. Soc. Am., **80**, 1188-1199.
6. S. Stannic, K.B. Briggs, P. Fleischer, R.I. Ray and W.B. Sawyer (1988) *Shallow water high frequency bottom scattering off Panama City, Florida*. J. Acoust. Soc. Am., **83**, 2134-2144.
7. S. Stannic, K.B. Briggs, P. Fleischer, W.B. Sawyer and R.I. Ray (1989) *High frequency acoustic backscattering from a coarse shell ocean bottom*. J. Acoust. Soc. Am., **85**, 125-136.
8. M.W. Lawrence, J.L. Thompson and M.J. Bell (1992) *Acoustic Bottom Backscatter measurements at High Frequencies*. Acoustics Australia, **20**, No. 3, 95-98.
9. R.E. Francois and G.R. Garrison (1982) *Sound absorption based on ocean measurements. Part I: Pure water and magnesium sulfate contributions; Part II: Boric acid contribution and equation for total absorption*. J. Acoust. Soc. Am., **72**, 896-907 and 1879-1890.

DISTRIBUTION LIST

FREQUENCY BOTTOM BACK SCATTERING IN THE DARWIN AREA

M. J. Bell

DSTO-TN-0048

AUSTRALIA

TASK SPONSOR:

DEFENCE ORGANISATION

Defence Science and Technology Organisation

Chief Defence Scientist
FAS Science Policy
AS Science Industry and External Relations
AS Science Corporate Management } shared copy
Counsellor Defence Science, London (Doc Data Sheet)
Counsellor Defence Science, Washington (Doc Data Sheet)
Scientific Adviser to MRDC Thailand (Doc Data Sheet)
Senior Defence Scientific Adviser/Scientific Adviser Policy and Command (shared copy)
Navy Scientific Adviser
Scientific Adviser - Army (Doc Data Sheet and distribution list)
Air Force Scientific Adviser
Director Trials

Aeronautical and Maritime Research Laboratory

Director

Electronics and Surveillance Research Laboratory

Director

Chief, Maritime Operations Division
Research Leader Operational Environment
Mr. J. L. Thompson
Mr. M. J. Bell

DSTO Library and Archiving

Library Fishermens Bend
Library Maribyrnong
Library Salisbury (2 copies)
AustralianArchives
Library, MOD, Pyrmont (2 copies)

Defence Central

OIC TRS, Defence Central Library
Officer in Charge, Document Exchange Centre (DEC), 1 copy
US Defence Technical Information Centre, 2 copies
UK Defence Research Information Centre, 2 copies
Canada Defence Scientific Information Service, 1 copy
NZ Defence Information Centre, 1 copy
National Library of Australia, 1 copy
Defence Intelligence Organisation
Library, Defence Signals Directorate (Doc Data Sheet)

Army

Director General Force Development (Land), (Doc Data Sheet)
ABCA Office, G-1-34, Russell Offices, Canberra (4 copies)

Navy

Director General Force Development (Sea)
Minehunter Coastal Project Director
SO (Science), Director of Naval Warfare, Maritime Headquarters Annex, Garden
Island, NSW 2000. (Doc Data Sheet)

RAAF

Director General Force Development (Air), (Doc Data Sheet)

UNIVERSITIES AND COLLEGES

Australian Defence Force Academy
Library
Head of Aerospace and Mechanical Engineering
Senior Librarian, Hargrave Library, Monash University
Librarian, Flinders University

OTHER ORGANISATIONS

NASA (Canberra)
AGPS

ABSTRACTING AND INFORMATION ORGANISATIONS

INSPEC: Acquisitions Section Institution of Electrical Engineers
Library, Chemical Abstracts Reference Service
Engineering Societies Library, US
American Society for Metals
Documents Librarian, The Center for Research Libraries, US

INFORMATION EXCHANGE AGREEMENT PARTNERS

Acquisitions Unit, Science Reference and Information Service, UK
Library - Exchange Desk, National Institute of Standards and Technology, US

SPARES (10 copies)

Page classification: UNCLASSIFIED

DEFENCE SCIENCE AND TECHNOLOGY ORGANISATION DOCUMENT CONTROL DATA		1. PRIVACY MARKING/CAVEAT (OF DOCUMENT)			
2. TITLE High Frequency Bottom Back Scattering in the Darwin Area		3. SECURITY CLASSIFICATION (FOR UNCLASSIFIED REPORTS THAT ARE LIMITED RELEASE USE (L) NEXT TO DOCUMENT CLASSIFICATION) Document (U) Title (U) Abstract (U)			
4. AUTHOR(S) M. J. Bell		5. CORPORATE AUTHOR Aeronautical and Maritime Research Laboratory PO Box 4331 Melbourne Vic 3001			
6a. DSTO NUMBER DSTO-TN-0048		6b. AR NUMBER AR-009-768		6c. TYPE OF REPORT Technical Note	7. DOCUMENT DATE July 1995
8. FILE NUMBER 510/207/0263	9. TASK NUMBER NAV 92/256	10. TASK SPONSOR MHCPD	11. NO. OF PAGES 28	12. NO. OF REFERENCES 9	
13. DOWNGRADING/DELIMITING INSTRUCTIONS None			14. RELEASE AUTHORITY Chief, Maritime Operations Division		
15. SECONDARY RELEASE STATEMENT OF THIS DOCUMENT					
<p style="text-align: center;"><i>Approved for public release</i></p> <p>OVERSEAS ENQUIRIES OUTSIDE STATED LIMITATIONS SHOULD BE REFERRED THROUGH DOCUMENT EXCHANGE CENTRE, DIS NETWORK OFFICE, DEPT OF DEFENCE, CAMPBELL PARK OFFICES, CANBERRA ACT 2600</p>					
16. DELIBERATE ANNOUNCEMENT					
No limitations					
17. CASUAL ANNOUNCEMENT Yes					
18. DEFTEST DESCRIPTORS					
Active sonar; Reverberation; Backscattering; Grazing angle; Sediment composition					
19. ABSTRACT <p>The backscatter of acoustic energy from the sea floor has been measured at acoustic frequencies of 34 kHz, 100 kHz and 205 kHz. Measurements made at several sites near Darwin are reported. Measurements were made as a function of grazing angle and azimuth. During the experiments site environmental measurements were made to characterise in detail the area of the acoustic measurements. The locations, equipment and techniques used during the measurements are described.</p>					

Page classification: UNCLASSIFIED